VOL. 3, NO. 7, July 2012 ISSN 2079-8407
Journal of Emerging Trends in Computing and Information Sciences
©2009-2012 CIS Journal. All rights reserved.
http://www.cisjournal.org

Design and Simulation of Miniaturized Minkowski Fractal Aperture-Coupled Antenna for 5.8 GHz RFID Applications

[1] D. K. Naji, [2] J. S. Aziz, [3] R. S. Fyath
Department of Electronic and Communications Engineering.,
College of Engineering, Al-Nahrain University, Baghdad, Iraq
[1] dknaji73@yahoo.com, [2] jsaziz53@yahoo.com, [3] rsfyath@yahoo.com

ABSTRACT

A miniaturized 3rd-order Minkowski fractal aperture-coupled antenna is designed for 5.8 GHz RFID applications using particle swarm optimization (PSO) technique. The PSO technique runs on MATLAB environment and synchronously coupled with an electromagnetic simulator (CST Microwave Studio) to estimate the radiation pattern parameters at each optimization iteration. Two objective functions are used to optimize the geometry of the antenna: return loss and the relative antenna size with respect to the reference (non-fractal) antenna. The simulated results show that the optimized fractal antenna has less than -37 dB return loss, more than 65% reduction in patch area and, more than 4 dB gains.

Keywords: *Aperture-coupled antenna, Minkowski fractal antenna, Particle swarm optimization, RFID.*

1. INTRODUCTION

Radio frequency identification (RFID) has excelled in automatic identification, bioengineering applications and data collection industry through its speed, agility, and endurance [1]. Recently, the operating frequency of RFID systems moves towards higher frequencies such as ISM band (5.8 GHz) to achieve higher identification range with higher data transfer rate [2]. This motivates researchers to apply micro strip antenna technology for RFID systems to gain the advantages of low profile, light weight, small volume, and mass production [3, 4]. For micro strip patch antennas, aperture coupling is preferred to other feeding mechanisms as it offers greater design flexibility [5, 6]. Aperture coupling has considerable advantage as a feeding mechanism particularly in fractal designs where identifying a suitable feed position on such complex geometrical shapes is particularly difficult [7].

Miniaturization of micro strip patch antenna has been typically accomplished by a suitable loading. One common technique in loading is to modify basic patch shapes. Applying fractals to antenna elements allows for smaller size, multiband, and broad-band properties. This is the cause of widespread research on fractal antennas in recent years [8-10]. Fractal geometries have self-similarity and space-filling nature when applied to antenna design [11-13]; and they can realize multi-frequency and size-reducing features. Several fractal geometries have been explored for antennas with special characteristics, such as the Sierpinski monopole [14], Koch curves [15] and the tree monopole [16]. These fractal geometries verify that the fractal antenna has size-reducing features within limited space.

The design of RFID antenna is still a challenge for miniaturization system due to the limited available area. This paper presents feasibility study to design miniaturized aperture-coupled micro strip antenna for 5.8 GHz RFID applications. The antenna miniaturization is achieved through two phases. The first phase applies fractal geometry while the second phase adopts particle swarm optimization (PSO) technique to get further area reduction. The CST Microwave Studio is used during the optimization process as an electromagnetic (EM) simulator to extract the antenna performance parameters that enter the objective function.

2. DESIGN METHODOLOGY

Particle swarm optimization algorithm has been tested by different research groups to different benchmark functions and results show that it is an excellent global optimizer that can be used for different electromagnetic problems especially antenna miniaturization [17, 18]. To calculate the antenna fitness function associated with the PSO algorithm, a comprehensive numerical modeling must be carried out to simulate the EM performance of the antenna at each iteration of optimization. The EM model should be very efficient in both speed of computation and accuracy since the geometry of the fractal antenna is relatively more complicated than the conventional counterpart and the dimensions of some structure parameters are much smaller than the operating wavelength. The required EM model features are recovered in this paper by using a commercial EM simulator namely CST MWS. This simulator uses finite integration time domain (FITD) method to assign the EM properties of antennas and has been proven in the literature as a powerful and very accurate tool for this purpose.

In this work, the fractal RFID antenna is optimized using PSO technique while the FITD method is used in parallel with it to compute the EM part of the fitness function (see Fig. 1). The PSO technique runs under MATLAB environment and the FITD method is offered by CST MWS software package. For each generation of the PSO algorithm, the antenna geometrical parameters are updated and mapped to CST MWS to simulate the EM properties of the antenna. According to the EM simulator

©2009-2012 CIS Journal. All rights reserved.

results that mapped back to MATLAB environment, the fitness function is evaluated by the PSO kernel.

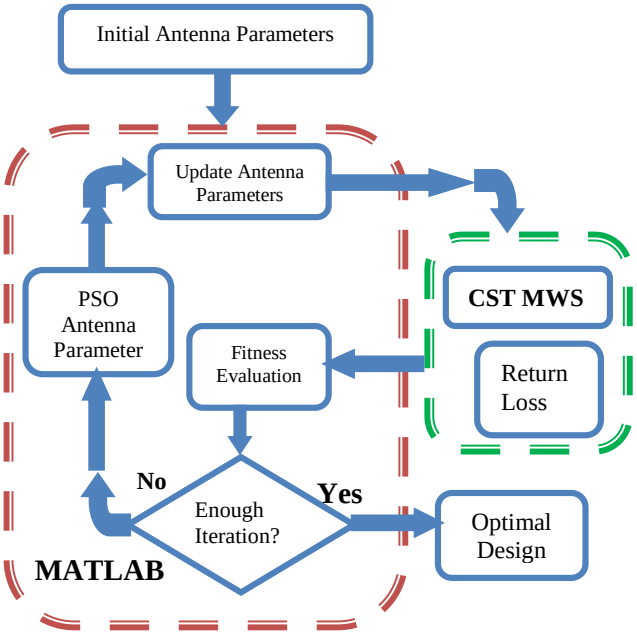

Fig 1: Data flow of the PSO/FITD algorithm.

The goal for the electromagnetic miniaturization design considered here is to minimize the size of the fractal antenna by altering the geometrical parameters within allowed prescribed ranges while keeping the return loss below a desired threshold value $(S_{11})_{th}$ at the required resonance frequency f_r. A suitable optimization model is Minimize the fitness function

$$\text{Fit}(x) = \left(S_{11\,at\,f_r} - (S_{11})_{th}\right) \cdot u\left(S_{11\,at\,f_r} - (S_{11})_{th}\right) + \left(\frac{A_F}{A_R} - 1\right) \quad (1)$$

Subject to $A_F < A_R$

and the constraints: $x_i^l \le x_i \le x_i^u$, $i = 1, 2, \ldots, N$

where

$$S_{11\,at\,f_r} = 20\,log\left|\frac{Z_{in\,at\,f_r} - Z_o}{Z_{in\,at\,f_r} + Z_o}\right| (dB) \quad (2)$$

In eqn. (1), u refers to the Heaviside step function while A_F and A_R denote, respectively, the area of the fractal and reference antennas. In eqn. (2), $S_{11\,at\,f_r}$ and $Z_{in\,at\,f_r}$ refer, respectively, to the return loss and the input impedance of the antenna at the resonance frequency f_r, and Z_o is the characteristic impedance ($Z_o = 50\Omega$).

Note that the optimization fitness function eqn. (1) consists of two objective functions which are related to antenna return loss S_{11} and antenna area.

$$Fit = obj_{S_{11}} + obj_{Area} \quad (3a)$$

Where

$$obj_{S_{11}} = \left(S_{11\,at\,f_r} - (S_{11})_{th}\right) \cdot u\left(S_{11\,at\,f_r} - (S_{11})_{th}\right) \quad (3b)$$

and

$$obj_{Area} = \left(\frac{A_F}{A_R} - 1\right) \quad (3c)$$

where $obj_{S_{11}}$ and obj_{Area} denote the return loss and area objective functions, respectively.

The objective function $obj_{S_{11}}$ represents the amount of matching at the desired frequency f_r and its value between "0" and "$-(S_{11})_{th}$". Its zero value denotes that the goal is achieved, that is to say a return loss of at least $(S_{11})_{th}$ at the desired frequency f_r is satisfied. The objective function obj_{Area} is used to achieve a minimum area from the optimization process. The range of obj_{Area} is between $(0, -1)$; it is zero if the area of the fractal antenna is equal to the area of the $reference$ counterpart, and to "-1" when the area of the fractal antenna is zero (not physically allowed). Thus the value of the total fitness function "Fit" which is considered as multiobjective optimization problem ranges between minimum values of "-1" to a maximum value of "$-(S_{11})_{th}$".

The antenna miniaturization methodology for the fractal micro strip antenna is performed using the following three steps

a. Design a conventional (non-fractal) aperture-coupled micro strip antenna using CST MWS. The dimensions of the structure parameters are tuned to achieve the design requirements ($S_{11} \le (S_{11})_{th}$) at the desired resonance frequency f_r. This antenna will be considered as a reference antenna (RA) for the design of the 3rd-order fractal antenna and its area is denoted by A_R.
b. Introduce the 3rd-order Minkowski geometry on the RA (see Fig. 2).
c. The 3rd-order fractal antenna (MFA3) is optimized with respect to the reference antenna according to the fitness function defined in eqn. (1).

3. DESIGN OF MINIATURIZED MINKOWSKI FRACTAL APERTURE-COUPLED ANTENNA

3.1. Reference Antenna

An aperture coupled micro strip patch structure having square ground plane ($L_g = W_g = 20\,mm$) is used as the reference (RA) (see Fig. 3). For the RA, the basic formulas for determining the length L_p and width W_p of the microstrip patch are [19]

VOL. 3, NO. 7, July 2012 ISSN 2079-8407
Journal of Emerging Trends in Computing and Information Sciences
©2009-2012 CIS Journal. All rights reserved.
http://www.cisjournal.org

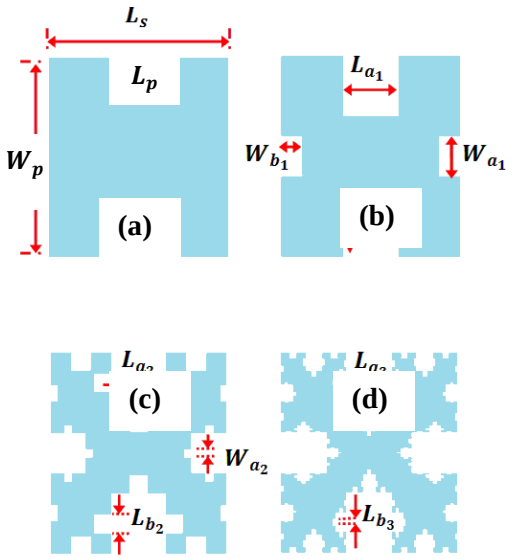

Fig 2: Scheme of the Minkowski fractal geometry (a) zero order (b) 1st order (c) 2nd order (d) 3rd order.

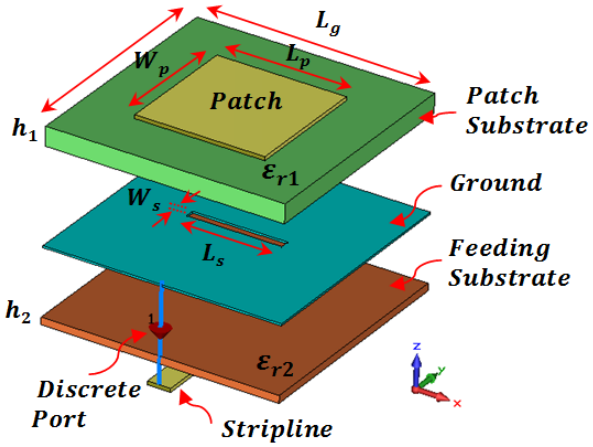

Fig 3: Aperture coupled-patch antenna.

.

$$W_p = \frac{c}{2f_r}\sqrt{\frac{2}{\varepsilon_r + 1}} \quad (4)$$

$$\varepsilon_{eff} = \frac{\varepsilon_r + 1}{2} + \frac{\varepsilon_r - 1}{2}\left(\frac{1}{\sqrt{1 + 12h_1/W_p}}\right) \quad (5)$$

$$\Delta L_p = 0.412\, h_1 \frac{\left(\varepsilon_{eff} + 0.300\right)\left[\frac{W_p}{h_1} + 0.264\right]}{\left(\varepsilon_{eff} - 0.258\right)\left[\frac{W_p}{h_1} + 0.813\right]} \quad (6)$$

$$L_p = \frac{c}{2f_r\sqrt{\varepsilon_{eff}}} - 2\Delta L \quad (7)$$

where W_p is the patch width, L_p is the patch length, ΔL_p is the patch length reduced from the patch antenna to reduce fringing effects, ε_r is the dielectric constant, c is the speed of wave in free space, and ε_{eff} is the effective dielectric constant. Using eqns. 4-7, the patch antenna is designed using Rogers 5880 substrate for patch and feed with dielectric constant $\varepsilon_r = 2.2$ and loss tangent of 0.0009. Table 1 illustrates the designed parameters of the reference aperture-coupled antenna at 5.8 GHz.

Table 1: Designed reference antenna geometrical parameters to achieve $f_r = 5.8\ GHz$.

Parameter	Symbol	Value (mm)
Ground length	L_g	20.00
Ground width	W_g	20.00
Patch length	L_p	14.50
Patch width	W_p	14.50
Stripline length	L_{st}	15.30
Ground slot length	L_s	7.00
Ground slot width	W_s	1.11
Patch substrate height	h_1	1.60
Feeding substrate height	h_2	0.80

3.2 Third-order Minkowski Fractal Antenna

In this subsection, a 3rd-order Minkowski fractal aperture-coupled antenna (MFA3) is optimized at $5.8\ GHz$ resonance frequency after miniaturizing the patch for fixed ground plane of size ($20\ mm \times 20\ mm$), see Fig. 2. Its shown from this figure that eight geometrical parameters enters the optimization process, five describing the patch side (patch length L_p and fractal scales parameters K_{L_a}, K_{L_b}, K_{W_a}, and K_{W_b}), two for the ground side (aperture slot length L_s and width W_s). The remain parameter is strip line length L_{st} related to the feeding side. In the optimization process, all the eight geometrical parameters are scaled version from ground length L_g ($W_g = L_g$) as

$$L_p = W_p = K_{L_p} \times L_g \quad (8a)$$

$$L_s = K_{L_s} \times L_p = K_{L_p} \times K_{L_s} \times L_g \quad (8b)$$

$$W_s = K_{W_s} \times L_p = K_{W_s} \times K_{L_p} \times L_g \quad (8c)$$

$$L_{st} = K_{L_{st}} \times L_p + 0.5L_g$$

$$= K_{L_{st}} \times K_{L_p} \times L_g + 0.5L_g \quad (8d)$$

©2009-2012 CIS Journal. All rights reserved.

The fractal scaling factors are introduced here for any fractal order. For 3rd-orer geometry, these four scaling factors are K_{L_a}, K_{L_b}, K_{W_a}, and K_{W_b} defined as follows

$$L_a^{(n)} = \left(K_{L_a}\right)^n \times L_p \quad (9a)$$

$$L_b^{(n)} = \left(K_{L_b}\right)^n \times W_p \quad (9b)$$

$$W_a^{(n)} = \left(K_{W_a}\right)^n \times W_p \quad (9c)$$

$$W_b^{(n)} = \left(K_{W_b}\right)^n \times L_p \quad (9d)$$

$$n = 1, 2, \ldots, n_{des}$$

where

$$L_{a1} = L_a^{(1)},\ L_{a2} = L_a^{(2)},\ L_{a3} = L_a^{(3)} \quad (10a)$$

$$L_{b1} = L_b^{(1)},\ L_{b2} = L_b^{(2)},\ L_{b3} = L_b^{(3)} \quad (10b)$$

$$W_{a1} = W_a^{(1)}, W_{a2} = W_a^{(2)},\ W_{a3} = W_a^{(3)} \quad (10c)$$

$$W_{b1} = W_b^{(1)}, W_{b2} = W_b^{(2)},\ W_{b3} = W_b^{(3)} \quad (10d)$$

The optimization model of eqn. (1) is applied here in order to miniaturize patch size while keeping the ground size fixed as ($20mm \times 20mm$).

The constraints used in the optimization process for the geometrical parameters are illustrated in Table 2

Table 2: Design parameter constraints used for optimizing MFA3.

Parameter	Symbol	Ranges
Patch length scale	K_{L_p}	0.10 ~ 0.72
Ground slot length scale	K_{L_s}	0.25 ~ 1.25
Ground slot width scale	K_{W_s}	0.05 ~ 0.25
Stripline length scale	$K_{L_{st}}$	0.00 ~ 0.6
Fractal patch length scale 1	K_{L_a}	0.10 ~ 0.33
Fractal patch length scale 2	K_{L_b}	0.20 ~ 0.33
Fractal patch width scale 1	K_{W_a}	0.10 ~ 0.33
Fractal patch width scale 2	K_{W_b}	0.20 ~ 0.33

The number of particles used here is 32, i.e., 4 particles for each of the eight geometrical parameter. Furthermore, a stop criterion is chosen such that 50 PSO iterations are reached or the fitness function remains unchanged with less than 2% error for at least 20 successive iterations.

4. RESULTS AND DISCUSSION

Illustrative results related to the design of a third-order Minkowski fractal antenna are given here. The threshold value of S_{11}, $(S_{11})_{th}$, used in the fitness function is $-25\ dB$. Figure 4 reveals that the progress of the PSO algorithm as a function of iteration number. Return loss and area objective functions as well total fitness function is illustrated in this figure.

The PSO algorithm creates an optimal miniaturized patch antenna size. Table 3 summarizes the final optimized geometrical parameters.

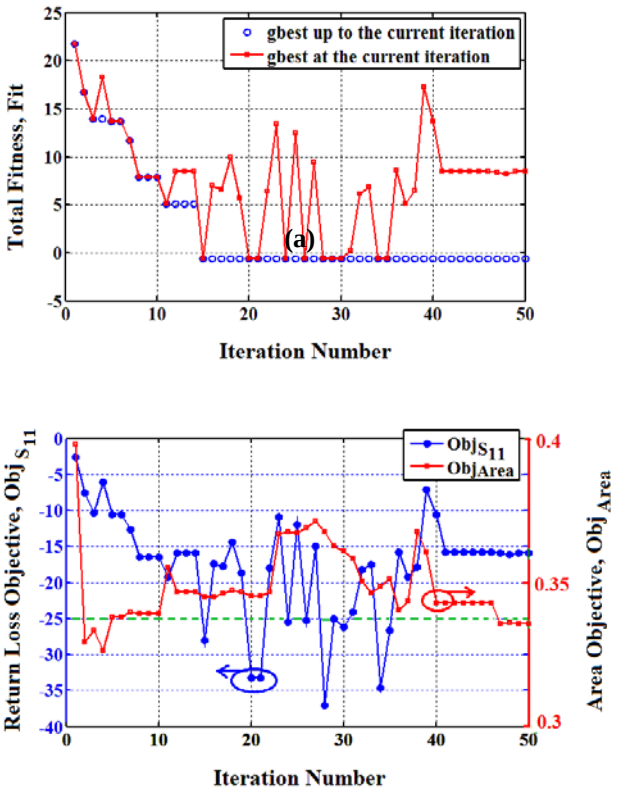

Fig 4: Variation of objective function with PSO iteration number for MFA3 (a) total (b) return loss and area.

Table 3: Optimized geometrical parameters of MFA3.

Parameter	Value
K_{L_p}	0.426
K_{L_s}	1.060
K_{W_s}	0.190
$K_{L_{st}}$	0.208
K_{L_a}	0.169
K_{L_b}	0.258
K_{W_a}	0.247
K_{W_b}	0.276

The performance results of the optimized MFA3 are carried out from the electromagnetic simulator CST. Table 4 lists some of the simulation results, namely, return

©2009-2012 CIS Journal. All rights reserved.

loss S_{11}, antenna gain G, total antenna efficiency η, bandwidth BW, and patch size reduction ΔA_p. The size Reduction is computed as

$$\Delta A_p = \frac{A_F - A_R}{A_R} \quad (11)$$

Table 4: Simulation results of optimized MFA3 and RA.

Antenna Performance Parameters	Antenna Type	
	RA	MFA3
S_{11} (dB)	-56.96	-37.37
G (dB)	6.08	4.48
η (%)	96.25	96.25
BW (GHz)	0.24	0.24
f_L (GHz)	5.696	5.68
f_H (GHz)	5.93	5.92
A_p (mm^2)	210.35	72.55
ΔA_p (%)	–	65.51

Investigating the results in Table 4 reveals that

a. The area of the optimized fractal patch antenna is equal to 34.5% of the area of the reference antenna.
b. A return loss less than $-37\ dB$, gain greater than $4.4\ dB$, and efficiency greater than 96% are obtained from RA and MFA3
c. Both RA and MFA3 have the same bandwidth ($240\ MHz$ at $-10\ dB$). Also, the lower and upper frequencies are nearly the same for the two antennas.

The return losses of optimized MFA3 together with reference counterpart are illustrated in Fig. 5. The two curves are almost the same over the whole frequency regions. Figures 6a and 6b show, respectively, the gain and efficiency for the designed antennas. It is clear from these figures that the 3rd-order fractal has almost similar spectral behavior.

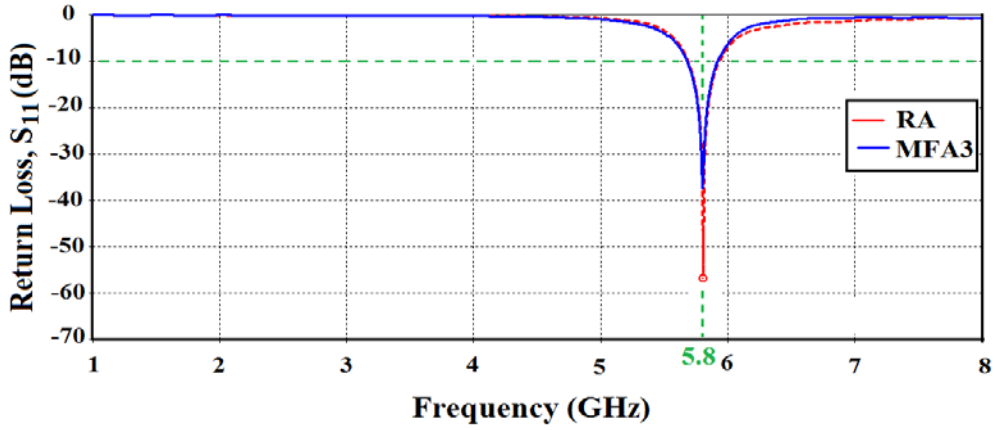

Fig 5: Simulated return losses of the optimized antenna. Results related to the reference antenna are given for comparison purposes.

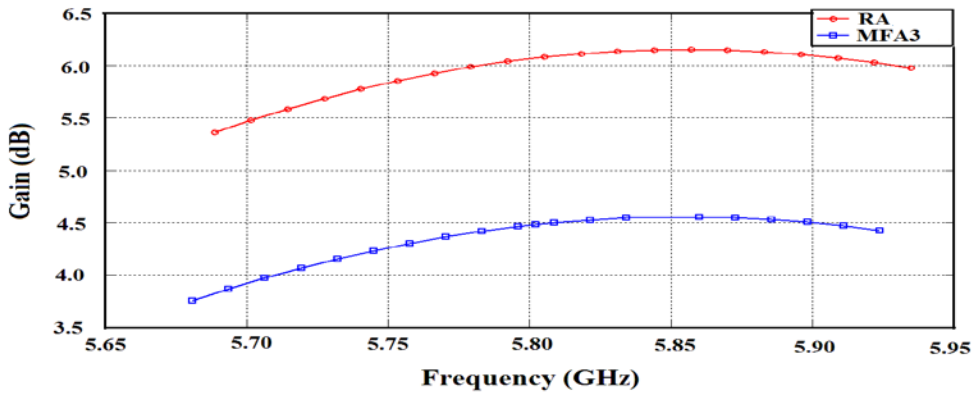

(a)

Fig 6: Gain (a) and efficiency (b) of the optimized fractal antenna. Results related to the reference antenna are also given.

©2009-2012 CIS Journal. All rights reserved.

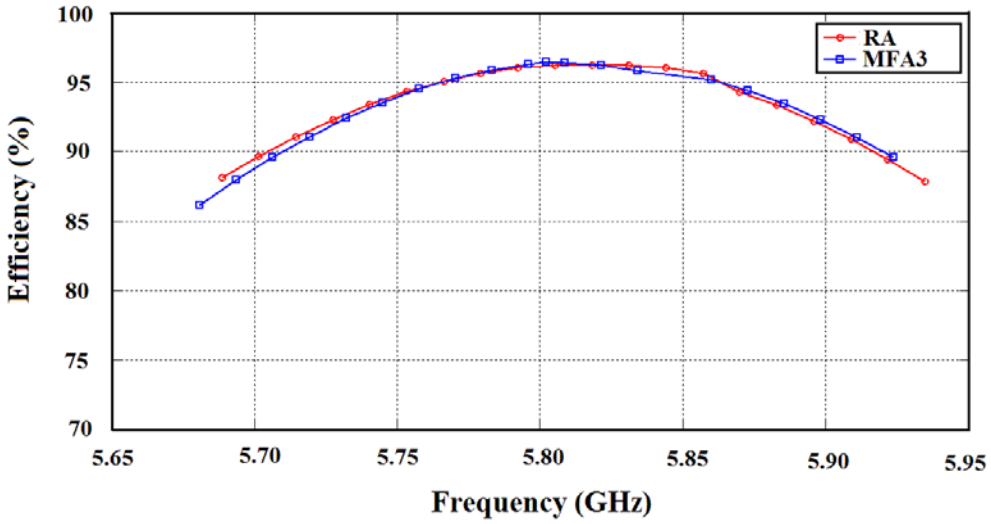

(***b***)

Fig 6: (Continued.)

The surface current distributions of RA and MFA3 antenna are displayed in Fig. 7. One can depict from this figure that the radiation is achieved from the vertical (width) side of the two antennas since the currents induces in the two vertical sides are of the same amplitude and direction. The radiation from horizontal (length) side is less from the vertical side because the currents in the two horizontal sides are of opposite direction and having different amplitudes. Thus, the width side has more effect on radiation than the length side. In other words, the width of patch antenna represents radiation side while the length of patch antenna represents resonance side.

The 3D radiation patterns of the two antennas are displayed in Fig. 8. It's shown that radiation patterns of the two antennas are almost the same. Figure 9 shows the radiation pattern in the elevation direction $\boldsymbol{yz}$ ($\emptyset = \mathbf{90}°$) and $\boldsymbol{xy}$ ($\boldsymbol{\theta} = \mathbf{90}°$) planes and azimuth direction $\boldsymbol{xz}$ ($\emptyset = \mathbf{0}°$) plane at $\mathbf{5.8}\,\boldsymbol{GHz}$ for the antennas. It is appears that the fractal antenna radiates nearly omni directionally. The radiation patterns show two nulls for $\mathbf{E_\theta}$ component at $\boldsymbol{\theta} = \mathbf{0}°$ and $\boldsymbol{\theta} = \mathbf{180}°$ for **xz**- and **xy**-plane, respectively, and two nulls for $\mathbf{E_\emptyset}$ component at $\emptyset = \mathbf{90}°$ and $\emptyset = -\mathbf{90}°$ for **xz**- and **xy**- planes, respectively.

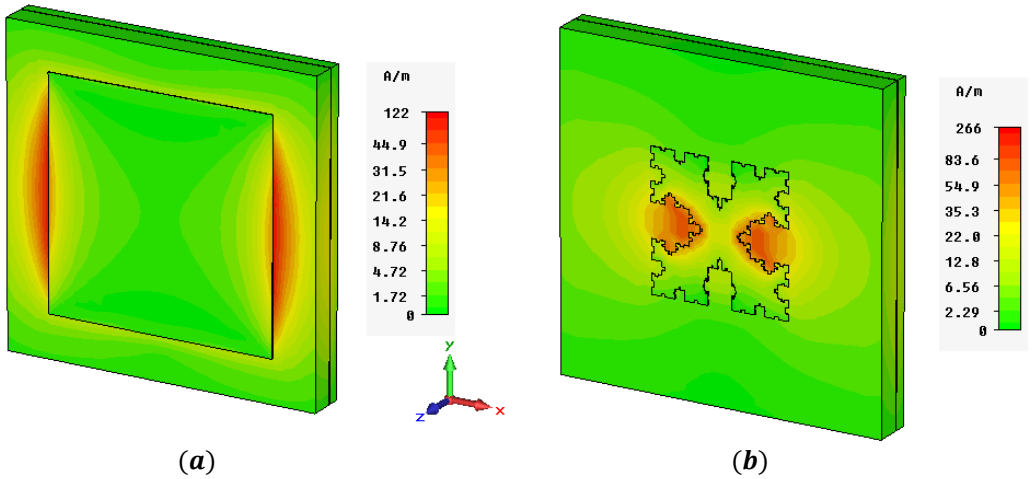

(***a***) (***b***)

Fig 7: Current distribution on antenna surface; (a) RA (b) MFA3.

©2009-2012 CIS Journal. All rights reserved.

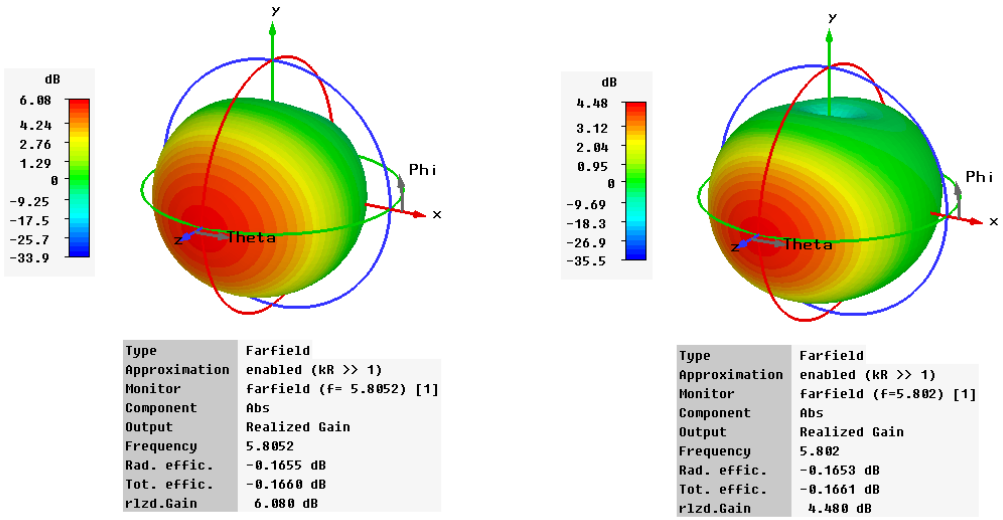

(a) (b)

Fig 8: 3D Radiation patterns for the Minkowski fractal aperture antenna; (a) RA (b) MFA3.

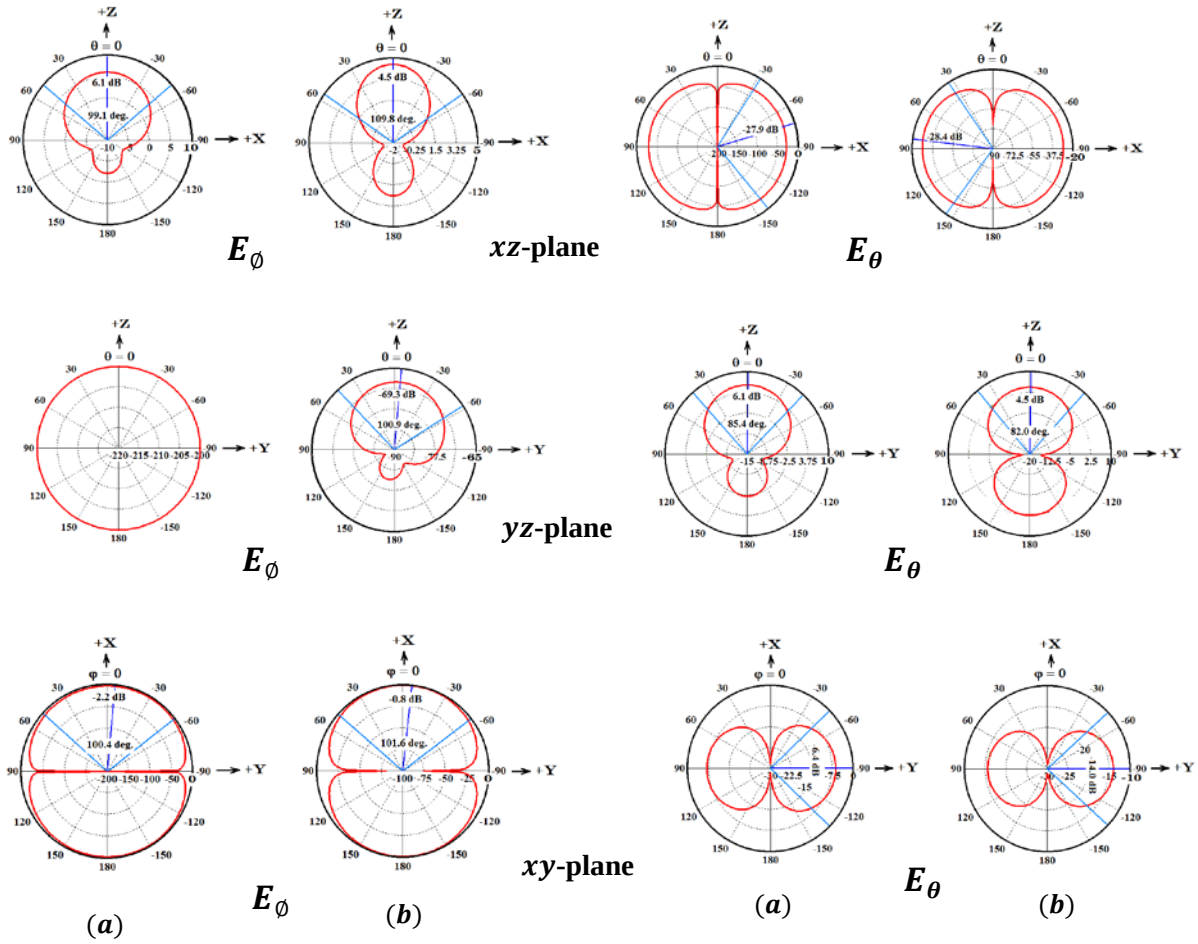

Fig 9: Radiation patterns for the Minkowski fractal aperture antenna; (a) RA (b) MFA3.

©2009-2012 CIS Journal. All rights reserved.

5. CONCLUSION

A miniaturized Minkowski fractal aperture-coupled antenna for 5.8 GHz RFID applications has been designed and investigated. The antenna geometrical parameters are optimized using PSO algorithm which runs on MATLAB environments and synchronously coupled to full wave electromagnetic simulator implemented using CST Microwave Studio software. The used optimization objective functions reflect both return loss and antenna size. The results reveals that more than 65% reduction in patch antenna size with fixed ground plane can be obtained as compared with the conventional reference antenna. Further, excellent performance requirements have been obtained with less than -37 dB return loss and more than 4 dB gain associated stable radiation pattern.

REFERENCES

[1] G. Marrocco, "RFID Antennas for the UHF Remote Monitoring of Human Subjects", IEEE Transaction on Antennas and Propagation, vol. 55, no. 6, pp.1862-1870, June 2007.

[2] A. T. Mobashsher, M. T. Islam, and N. Misran, "A Novel High-Gain Dual-Band Antenna for RFID Reader Applications'', IEEE Antennas and Wireless Propagation Letters, vol. 9, pp. 653-655, July 2010.

[3] I-F. Chen and C.-M. Peng, "A Novel Reduced-Size Edge-Shorted Patch Antenna for UHF Band Applications", IEEE Antennas and Wireless Propagation Letters, vol. 8, pp. 475-477, 2009.

[4] D. Guha and Yahia M. M. Antar, "Microstrip and Printed Antennas New Trends, Techniques and Applications", New York: Wiley, 2011.

[5] S. Chakrabarti , "Development of Shared Aperture Dual Polarized Microstrip Antenna at L-Band", IEEE Transactions on Antennas and Propagations ,vol. 59, no. 1, pp. 294-297, Jan. 2011.

[6] B. Ghosh, S. N. Sinha, and M. V. Kartikeyan "Radiation From Rectangular Waveguide-Fed Fractal Apertures" ", IEEE Transactions on Antennas and Propagations, vol. 58, no. 6, pp. 2088-2093, June 2010.

[7] S. N. Sinha, and M. Jain, "A Self- Affine Fractal Multiband Antenna," IEEE Antennas and Wireless Propagation Letters, vol. 6, pp. 110-112, 2007.

[8] Y. J. Sung, "Bandwidth Enhancement of a Wide Slot Using Fractal-Shaped Sierpinski", IEEE Transactions on Antennas and Propagations, vol. 59, no. 8, pp. 3076-3079, Aug. 2011.

[9] H. Kimouche, H. Zemmour, and B. Atrouz, "Dual-band fractal shape antenna design for RFID applications", Electronics Letters, vol. 45, no. 21, pp. 1061-1063, Oct. 2009.

[10] M. N. Jahromi, A. Falahati, and R. M Edwards, "Bandwidth and Impedance-Matching Enhancement of Fractal Monopole Antennas Using Compact Grounded Coplanar Waveguide", IEEE Transactions on Antennas and Propagations ,vol. 59, no. 7, pp. 2480-2487, July 2011.

[11] D. H. Werner and S. Ganguly, "An Overview of Fractal Antenna Engineering Research," IEEE Antenna and Propagation Magazine, vol. 45, no. 1, pp. 38-57, Feb. 2003.

[12] K. J. Vinoy, J. K. Abraham, and V. K. Vardan, "On the Relationship Between Fractal Dimension and the Performance of Multi-Resonant Dipole Antennas using Koch Curves," IEEE Transactions on Antennas and Propagations, vol. 51, no. 9, pp. 2296 – 2303, Sept. 2003.

[13] S. H. Zainud-Deen, H. A. Malhat, and K. H. Awadalla, "Fractal Antenna for Passive UHF RFID Applications", Progress In Electromagnetics Research B, Vol. 16, 209-228, 2009.

[14] W. J. Krzysztofik, "Modified Sierpinski Fractal Monopole for ISM-Bands Handset Applications", IEEE Transaction on Antennas and Propagation, vol. 57, no. 3, pp. 606-615, Mar. 2009.

[15] K. J. Vinoy, J. K. Abraham, and V. K. Varadan, "A Koch-Like Sided Fractal Bow-Tie Dipole Antenna", IEEE Transactions on Antennas and Propagations ,vol. 60, no. 5, May 2012.

[16] H. Rmili, O. E. Mrabet,J. –M. Floc'h, and J.-L. Mian, " Study of an Electrochemically-Deposited 3-D Random Fractal Tree-Monopole Antenna", IEEE Transaction on Antennas and Propagation, vol. 55, no. 4, pp. 1045-1050, April 2007.

[17] J. Nanbo, and Y. Rahmat-Samii, "Advances in particle Swarm Optimization for Antenna Designs: Real-Number, Binary, Single-Objective and Multiobjective implementation", IEEE Transaction on Antennas and Propagation, vol. 55, no. 3, Mar. 2007.

[18] J. Nanbo, and Y. Rahmat-Samii, "Hybrid Real-Binary Particle Swarm Optimization (HPSO) in Engineering Electromagnetics", IEEE Transaction on Antennas and Propagation, vol. 58, No. 12, Dec. 2010.

[19] C. A. Balanis, Antenna Theory: Analysis and Design, 3rd ed. Hoboken, NJ: Wiley, 2005.